DOI: 10.1002/chem.200902253

Hydroxylation and Ring-Opening Mechanism of an Unusual Flavoprotein Monooxygenase, 2-Methyl-3-hydroxypyridine-5-carboxylic Acid Oxygenase: A Theoretical Study

Boxue Tian,[a, b] Yaoquan Tu,[a] Åke Strid,[a] and Leif A. Eriksson*[a, b]

Abstract: Hybrid meta-GGA density functional theory (the MPWB1K functional) was used to study the hydroxylation and ring-opening mechanism of 2-methyl-3-hydroxypyridine-5-carboxylic acid oxygenase (MHPCO). This enzyme catalyses the conversion of 2-methyl-3-hydroxypyridine-5-carboxylic acid (MHPC) to α-(*N*-acetylaminomethylene)succinic acid (AAMS), which is the essential ring-opening step in the bacterial degradation of vitamin B_6. MHPCO belongs to the flavin-containing aromatic hydroxylases family. However, MHPCO is capable of catalysing a subsequent aromatic ring-cleavage reaction to give acyclic products rather than hydroxylated aromatic ones. Our calculations show that the re-aromatisation of the hydroxylated intermediate occurs spontaneously in aqueous solution; this implies that the ring-opening process occurs inside the enzyme's active site, in which limited water is available. The instability of the hydroxylated intermediate of MHPCO is the main reason why acyclic products are formed. Previously proposed mechanisms for the ring-opening step were studied, and were shown to be less likely to occur ($\Delta\Delta G^{\neq 298} > 35$ kcal mol^{-1}). Two new pathways with reasonable barrier heights ($\Delta\Delta G^{\neq 298} < 15$ kcal mol^{-1}) are reported herein, which are in accordance with all experimental information present to date.

Keywords: hydroxylation · flavoprotein monooxygenase · molecular modeling · ring-opening reactions · vitamins

Introduction

Flavoprotein monooxygenases (FMOs) are a group of enzymes capable of efficiently and regioselectively catalysing a large number of oxidative reactions.[1–5] Within the FMO family, the aromatic hydroxylases have received much attention over the last three decades, and the protein structures of some members have already been determined.[6–9] The aromatic hydroxylase enzymes are capable of hydroxylating aromatic rings at the *ortho* position of phenolic substrates via electrophilic aromatic substitution reactions.[10–12]

2-Methyl-3-hydroxypyridine-5-carboxylic acid oxygenase (MHPCO) is a unique member of this aromatic hydroxylase family because the reactions catalysed by the enzyme give acyclic products rather than aromatic ones.[13–18] So far, three compounds have been shown to be substrates of MHPCO, namely, 2-methyl-3-hydroxypyridine-5-carboxylic acid (MHPC), 5-hydroxynicotinic acid (5HN) and *N*-methyl-5-hydroxynicotinic acid (NMHN); see Equation (1).[19,20]

The conversion of MHPC to α-(*N*-acetylaminomethylene)succinic acid (AAMS) is the essential ring-opening step in the bacterial degradation of vitamin B_6. In the degradation, vitamin B_6 undergoes a series of initial bacterial oxidation and decarboxylation steps to give MHPC. After the ring cleavage, AAMS will further convert to ammonia, carbon dioxide, acetate and succinic semialdehyde, enabling the bacteria to use pyridoxine as its sole source of carbon and nitrogen (Supporting Information, S1).[21–24]

Investigating the catalytic mechanism of MHPCO is of great importance for the understanding of the aromatic hydroxylase family as well as further applications of such reactions in general.

Previous studies have shown that the monooxygenation process catalysed by aromatic hydroxylases can be divided into two parts: reduction and oxidation. In the reduction part, with NADPH and the substrate already bound, the FAD cofactor is reduced by NADPH. In the oxidation part,

[a] B. Tian, Dr. Y. Tu, Prof. Å. Strid, Prof. L. A. Eriksson
Örebro Life Science Center School of Science and Technology
Örebro University, 70182 Örebro (Sweden)

[b] B. Tian, Prof. L. A. Eriksson
School of Chemistry
National University of Ireland, Galway (Ireland)
Fax: (+353) 91-525700
E-mail: leif.eriksson@nuigalway.ie

Supporting information for this article is available on the WWW under http://dx.doi.org/10.1002/chem.200902253.

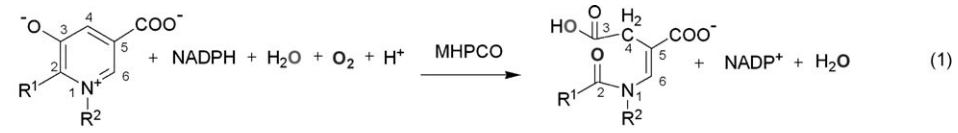

Substrates of MHPCO:
MHPC: $R^1 = CH_3$, $R^2 = H$
5HN: $R^1 = H$, $R^2 = H$
NMHN: $R^1 = H$, $R^2 = CH_3$

AAMS: $R^1 = CH_3$, $R^2 = H$

the reduced $FADH^-$ reacts with molecular oxygen to form C-(4a)-flavinhydroperoxide (FlHOOH), which is a short-lived intermediate (Supporting Information, S2).[25] FlHOOH then acts as an electrophile in the oxygenation, and the terminal hydroxyl group is transferred from FlHOOH to the substrate through electrophilic aromatic substitution.[10–12]

Previous experimental investigations have provided useful information on the catalytic mechanism of MHPCO. In the experimental studies of Chaiyen et al. several mechanisms were proposed.[19,20] Based on the crystal structure, McCulloch et al. recently proposed a new mechanism.[6] Although different pathways are suggested, they share the similarity that hydroxylation (Scheme 1) and ring opening are the two key catalytic steps (experiments were unable to differentiate between the different pathways). As with other aromatic hydroxylases, the substrate is first hydroxylated by C-(4a)-flavinhydroperoxide (FlHOOH) through an electrophilic aromatic substitution, which is the rate-limiting step. In the ring-opening step, a water molecule is added to the hydroxylated intermediate either before or after the C2–C3 bond cleaves [Eq. (1)].

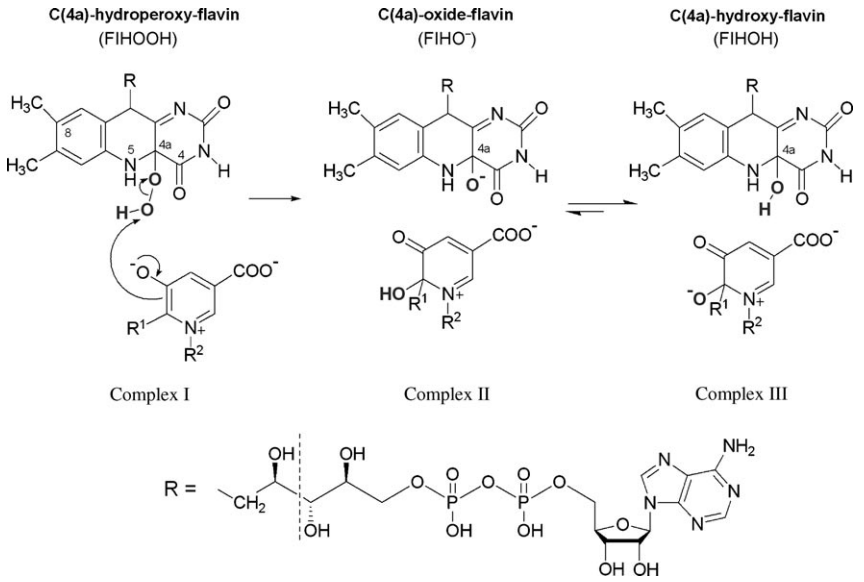

Scheme 1. Proposed hydroxylation step of MHPCO: In this paper, the ribityl chain was replaced by CH_2CH_2OH (at the dashed line).

So far, no theoretical study on the full catalytic process of MHPCO has been reported. However, there are some theoretical studies modelling the hydroxylation step of *p*-hydroxybenzoate hydroxylase (PHBH), a paradigm aromatic hydroxylase, which provides insight into the hydroxylation step.[26–33] In these studies, the energy barrier of the hydroxylation step was determined to be 20–30 kcal mol^{-1} by using different theoretical methods. Because the experimental value is 12 kcal mol^{-1}, it was suggested that additional interactions with the enzyme must be considered for the hydroxylation step.[26]

Based on previous experimental data, we have herein examined the catalytic mechanism of MHPCO by using quantum chemical methodology in the hybrid meta-GGA density functional theory framework. Previously proposed mechanisms were studied, and two new pathways are presented based on theoretical considerations.

Computational Methods

The hybrid meta density functional theory (HMDFT) method MPWB1K[34] was used to study the reaction pathways because MPWB1K is known to provide accurate barrier heights as well as hydrogen-bonding interactions.

Intermediates and transition states were first optimised in vacuo at the B3LYP/6-31G(d) level.[35–37] Further geometry optimisations by using MPWB1K/6-31+G(d,p) were performed on the geometries of the previous step, followed by frequency calculations at the same level of theory to ensure that these were stationary structures on their respective energy surfaces and to extract Gibbs free energy corrections at 298 K. Transition states were tested by using intrinsic reaction coordinate (IRC) calculations to make sure that they connected the correct reactants and products in each step. The integral equation formalism of the polarised continuum model (IEFPCM)[38,39] with UAHF radii was used to optimise geometries and calculate frequencies for all conversions that occur in aqueous solution ($\varepsilon = 78.3$).

Single-point energy calculations were performed on the optimised structures by using

the higher basis set 6-311+G(2d,2p) in the proton affinity calculation of the hydroxylated intermediates (see below). When evaluating the rotation barrier of different configurations, both transition states in clockwise and anticlockwise rotation were located, and the one with the lower energy barrier was chosen to be the transition state (TS).

The substrate 5HN was used instead of MHPC for all the calculations because 5HN is also a substrate of MHPCO and has fewer atoms; the difference between the two structures is a methyl group in the R^1 position [Eq. (1)]. This is, however, expected to influence the energetics of the reactions to a very small extent. All calculations were performed by using the Gaussian 03 program.[40]

Results and Discussion

Hydroxylation

Reactant complex: According to previous titration experiments, the substrates of MHPCO exist in their tripolar forms when binding to the enzyme [Eq. (2)].[20] It should be mentioned that in the related enzyme (PHBH) although the substrate *p*-hydroxybenzoate should not have the phenolic hydroxyl deprotonated at neutral pH, it has been shown to attain a phenolate form in the enzyme.[41] It was argued that, with the phenolic hydroxyl deprotonated, the substrate is in a higher energy form, thus the energy barrier for hydroxylation is lowered.[26] These enzymes thus activate the substrate by controlling its protonation state.

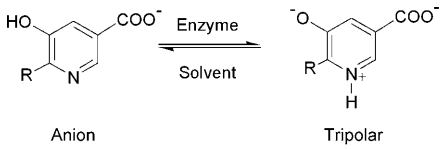

(2)

Comparing the energies and structures of the anion and tripolar forms of 5HN both in vacuo and in water (PCM), the Gibbs free energy of the anion form is found to be 11.9 kcal mol^{-1} lower than the tripolar form in vacuo, and 7.9 kcal mol^{-1} lower in water (see Figure 1). Therefore, 5HN exists mainly in the anion form in water. Compared with the anion form, the C2–C3 and C3–C4 bond lengths are increased in the tripolar form (1.384→1.424 Å and 1.381→1.439 Å), whereas the C3–O bond length is decreased (1.363→1.246 Å). Because these geometric features resemble those of the hydroxylated form, conversion of the substrate into the tripolar form predisposes this to facilitate hydroxylation.

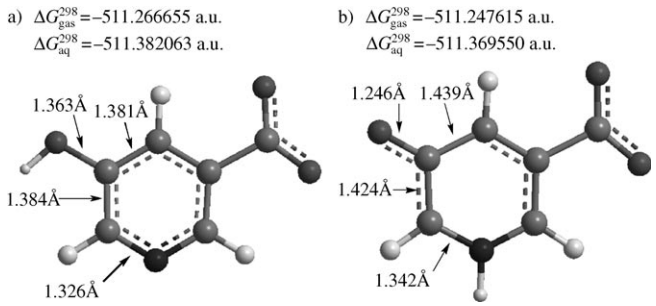

Figure 1. Optimised geometries a) the anion form and b) the tripolar form of 5HN in vacuo.

In the reactant complex (Complex **I**), we replaced the ribityl chain with an ethanolyl group (CH_2CH_2OH) to simplify the large system. The complexation energy, that is, the energy difference between the reactant complex (Complex **I**) and the isolated reactants (FlHOOH and tripolar 5HN), is −16 kcal mol^{-1}. Thus FlHOOH and 5HN readily form a reactant complex. In optimised complex **I**, the FAD and 5HN planes are essentially parallel to each other (Figure 2a). The hydroperoxyl group forms a hydrogen bond with the phenolic oxygen in 5HN, and the H···O distance is 1.630 Å. This interaction can have an effect on the barrier height of the subsequent hydroxyl transfer because in the transition state the H···O distance is 2.990 Å and the interaction thus much weaker (Figure 2b). It should be noted that the phenolic oxygen in 5HN also can form a hydrogen bond with the NH group of FlHOOH (H···O distance 1.939 Å, Figure 2a), but this interaction is not as strong as the interaction with the hydroperoxide group. However, this interaction can possibly affect the hydroxyl transfer because it becomes weaker in the product complex (H···O distance: 2.105 Å).

TS and product complex: In **TS I–II**, the C2–O and O–O distances are 1.908 and 1.768 Å, respectively (see Figure 2b). The geometry of **TS I–II** is similar to previous DFT studies on the corresponding reaction in PHBH.[26,27] However, we note that the imaginary frequency $\nu_i = 659.7i\ cm^{-1}$ obtained herein is higher than $\nu_i = \sim 400i\ cm^{-1}$ reported for the hydroxylation step of PHBH. A likely cause is the use of a different functional in the calculations, but slightly different geometric structures at the TS will also have an impact. In a previous comprehensive study on hydroperoxides, Bach and Dmitrenko[27] found that the imaginary frequency of a transition state can be used to estimate whether the oxidative reaction of the hydroperoxide is a hydroxyl transfer (corresponding to a low imaginary frequency) or a direct oxygen transfer process (corresponding to a high imaginary frequency). According to this result, the current oxygenation reaction with an imaginary frequency $\nu_i = 659.7i\ cm^{-1}$ is still a hydroxyl transfer process. The hydroxyl transfer, which gives complex **II**, shares similarity with an S_N2 reaction, with $FlHO^-$ as the leaving group.

We obtained an energy barrier of 33.8 kcal mol^{-1} for the hydroxylation reaction, which is higher than previous DFT studies by using the B3LYP method.[26] Albeit too high for an enzymatic reaction, it is consistent with the fact that B3LYP usually underestimates energy barriers, whereas the newer methods, such as MPWB1K, that are parametrised particularly for accurate evaluation of barrier heights, in

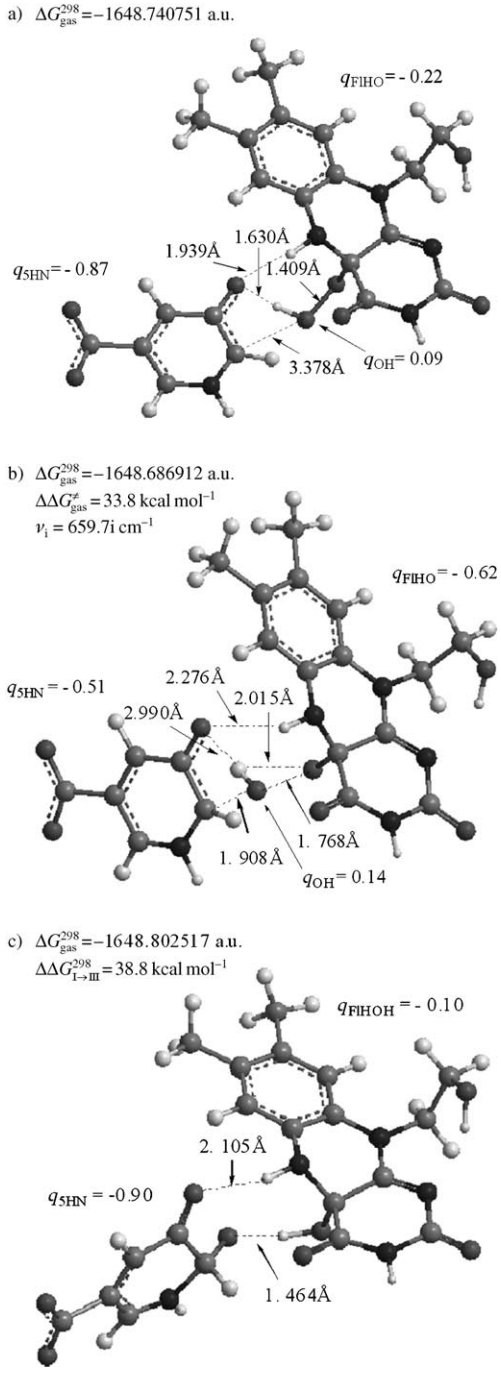

Figure 2. Optimised geometries of a) complex **I**, b) **TS I–II**, c) complex **III** in the hydroxylation step.

general provide higher values.[34] The too-high barrier found herein can largely be ascribed to the fact that no explicit active-site residues, which might stabilise the TS through hydrogen bonding or electrostatic interactions, were included.

When optimising the product complex, this immediately rearranges to complex **III** instead of **II** (Scheme 1 and Figure 2c). It is known that in this type of hydroxyl-transfer reaction, the final product complex of the hydroxylation step is determined by the proton affinity (PA) of $FlHO^-$ versus the hydroxylated intermediate.[26] The calculated PA values of $FlHO^-$ and compound **1** by using MPWB1K/6-311+G-(2d,2p) show that the PA of **1** (333 kcal mol^{-1}) is 12 kcal mol^{-1} lower than that of $FlHO^-$ (345 kcal mol^{-1}) [Eqns. (3) and (4)]. This implies that complex **III** will be more stable than **II**, in accordance with the spontaneous rearrangement found.

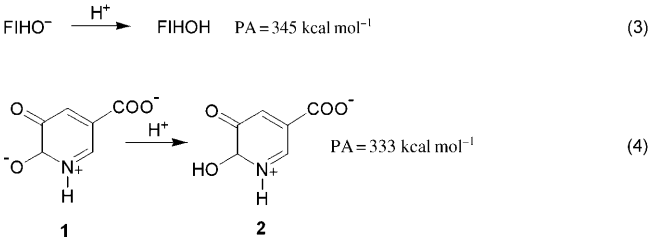

Reaction mechanism: Because the hydroxylation step is proposed to be an electrophilic aromatic substitution reaction,[13] we analysed the atomic charges of the complexes in the hydroxyl-transfer process. The transferred hydroxyl retains a nearly neutral state in the reactant and transition state. An electron is transferred from 5HN to $FlHO^-$ during the process, and in the transition state, the total atomic charges of the 5HN part and the $FlHO^-$ part are close to $-0.5\ e^-$ each (Figure 2), in accordance with an electrophilic aromatic substitution mechanism.

However, by using IRC calculations to trace the conversion of the transition state to the product complex, the hydroxyl is found to rotate before binding to the carbon atom of 5HN. In the rotation, the hydroxyl proton is transferred back to $FlHO^-$ to give product complex **III**. The energy surface for proton transfer from $FlHO^-$ to 5HN (i.e., from complex **III** to **II**) was scanned, showing that the reaction is strictly endothermic along the reaction coordinate, even as the O–H length in complex **II** reached 0.98 Å. However, the total energy difference is only 1.5 kcal mol^{-1}, which is much smaller than the PA difference (12 kcal mol^{-1}). This implies that the product complex is not simply determined by the PA values, and more factors must be considered. Therefore, we suggest that both complex **II** and **III** can be the product of the hydroxylation step, with complex **III** being slightly favoured (Scheme 1).

In the hydroxylation step, due to the S_N2-like reaction, a chiral carbon atom is formed. In the enzyme's active site pocket, the substrate will not be able to flip between different orientations (due to a hydrogen-bonding network stabilising the substrate), so we propose that there will be one stereoselective product in the hydroxylation step. In our calculation, product **1a** was formed [Eq. (5)] because the initial orientation was chosen from the crystal structure. Therefore, the *R* configurations of **1** (**1a**) and **2** (**1a** protonated) were used for the calculations below. It should be noted that the stereochemistry of compounds **1** and **2** does not affect the configuration of the product in these model calculations.

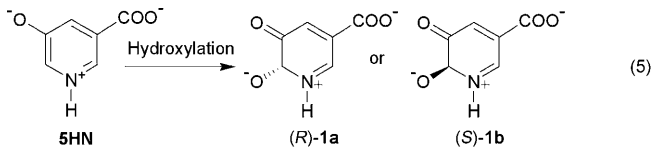

(5)

Ring cleavage

The role of enzyme structure: As mentioned above, MHPCO is an unusual member in the aromatic hydroxylase family because after the hydroxylation, there is a further ring-cleavage process to give an acyclic product instead of an aromatic one.

According to Chaiyen et al.,[19,20] the ring-opening process is faster than the rearomatisation so as to prevent the formation of the aromatic product. However, our calculations show that the C2–C3 bond strength in **2** is not that weak (> 40 kcal mol^{-1}). Moreover, when we optimised the geometry in water (optimisation with PCM model), the rearomatisation occurs spontaneously (Supporting Information, S3). To validate our discovery, we also studied the hydroxylated product of a typical aromatic hydroxylase, PHBH. The hydrogen on C2 readily leaves during the optimisation, and a charge distribution analysis shows that the leaving hydrogen carries a positive charge of 0.86e$^-$, that is, a proton. Thus we suggest that once the hydroxylated intermediate is released into aqueous solution, the rearomatisation occurs (Scheme 2). Hence, in the active site of MHPCO there should be a limited amount of water present around the substrate, and the hydroxylated intermediate is not released into water until the aromatic ring is cleaved. The enzyme structure study by McCulloch et al. shows that the active site pocket of MHPCO is significantly different from the other aromatic hydroxylases.[6]

Therefore, the uniqueness of MHPCO is determined by both the unstable hydroxylated intermediate and the particular protein structure.

Note that the rearomatisation of **1** and **2** can also occur by a typical enolisation reaction of the carbonyl group at C3. However, our calculations show that the energy barriers of this type of reaction are extremely high in vacuo for both **1** and **2** (82.5 kcal mol^{-1} for **1** and 61.6 kcal mol^{-1} for **2**, Supporting Information S4). We thus consider this type of reaction unlikely to occur in the enzyme active site.

Previous ring-opening pathways: In previous studies by Chaiyen et al, it was suggested that after the hydroxylation, with the FlHO$^-$ moiety leaving, the hydroxylated substrate (similar to **2**) undergoes the ring-cleavage reaction with the help of water.[19,20] Recently, McCulloch et al. proposed a new mechanism involving that the hydroxylated intermediate cleaves at the C2–C3 bond to give a ketene intermediate, which is further hydrated to the product.[6] Both mechanisms (Scheme 3) have been evaluated in vacuo (in water, **2** is not stable, as mentioned above).

Our calculations show that the pathway proposed by McCulloch et al. is very difficult to obtain (**2**→**3**, $\Delta\Delta G^{\neq 298}$ = 41.9 kcal mol^{-1}). The carboxyl group in **2** is out of the ring plane, implying a poor conjugation (Figure 3a). As we mentioned above, in the PCM optimisation the proton on C2

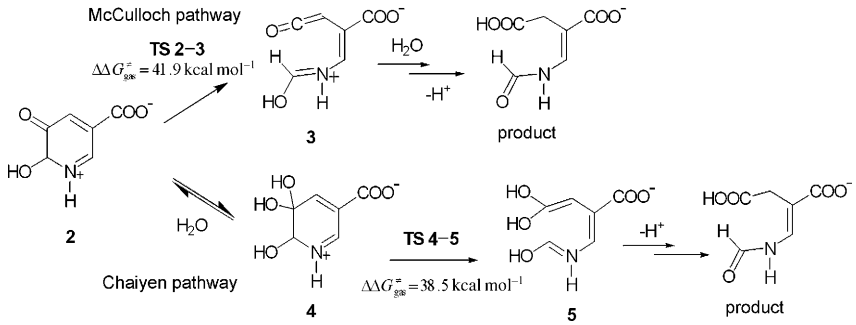

Scheme 3. Previous mechanisms of Chaiyen[19,20] and McCulloch.[6]

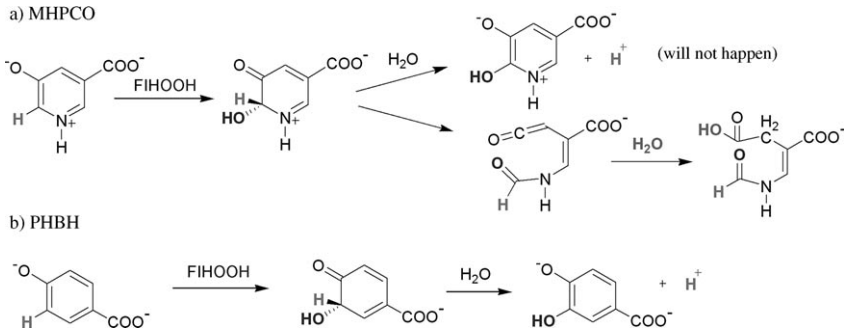

Scheme 2. Comparison of the pathways of MHPCO and a typical aromatic hydroxylase PHBH: a) Proposed reaction pathway of MHPCO with the substrate 5HN; b) Reaction pathway of PHBH with substrate *para*-hydroxybenzoate.

leaves the molecule directly and carries a net positive charge (rearomatisation). In vacuo, this positive charge is distributed mainly on C2 (q = 0.42e$^-$) and C4 (q = 0.68e$^-$) rather than on the nitrogen atom as described in the Lewis structure.[42] The bond lengths of N1–C2, C2–C3 and C3–C4 are 1.455, 1.526 and 1.451 Å, respectively (Figure 3a), which implies that the ring atoms in compound **2** are not conjugated to a delocalised system. The TS

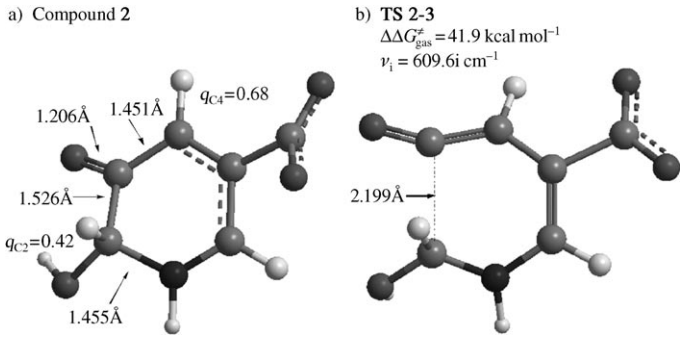

Figure 3. Optimised geometries of a) compound **2** and b) **TS 2–3** in vacuo.

has a C2–C3 bond length of 2.199 Å ($\Delta\Delta G^{\neq 298}$ = 41.9 kcal mol^{-1}, ν_i = 609.6i cm^{-1}). From reactant **2** to **TS 2–3**, the C2–C3 bond length is thus increased by 0.673 Å (Figure 3b). All the information suggests that this pathway will not occur.

According to Chaiyen et al., adding water to **2** gives **4**, which undergoes the ring-opening reaction.[19,20] Because we are interested in the ring-opening process, the energy barrier of the water addition was not considered. The carboxyl group is in the ring plane in **4**, implying a larger conjugation compared to **2**. The C2–C3 bond in **4** is 1.538 Å, slightly longer than that in **2**. The positive charges on C2 (q = 0.40e$^-$) and C4 (q = 0.62e$^-$) are reduced compared with **2** (Figure 4a). In **TS 4–5**, the distance between C2 and C3 is

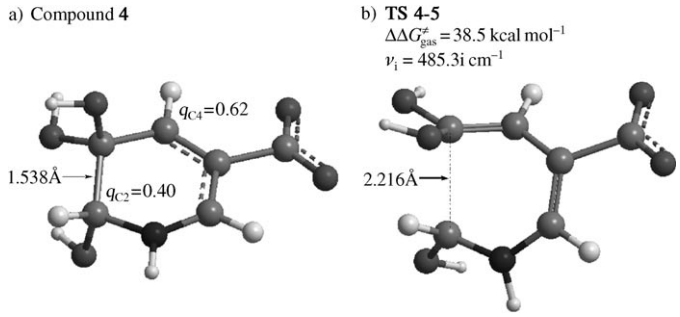

Figure 4. Optimised geometries of a) compound **4** and b) **TS 4–5** in vacuo.

2.216 Å, which is similar to that in **TS 2–3** (Figure 4b). The energy barrier for the ring-opening conversion of **4** to **5** (**TS 4–5**, $\Delta\Delta G^{\neq 298}$ = 38.5 kcal mol^{-1}, ν_i = 485.3i cm^{-1}) is 3.4 kcal mol^{-1} lower than that of **TS 2–3**. However, this value is still higher than that of hydroxylation, which is known to be the rate-limiting step. Therefore, Chaiyen's pathway is also less likely to give the ring-opened product.

Current ring-opening pathways: When using the favoured product of the hydroxylation step, compound **1**, we find two different pathways leading to the acyclic product (Scheme 4). Compared with Scheme 3, these two pathways display much lower barrier heights.

In pathway A, the C2–C3 bond length of **TS 1–6a** is increased to 1.864 Å, after which the ring cleaves to give the ketene intermediate **6a**. The energy barrier of the reaction is 14.1 kcal mol^{-1} (**TS 1–6a**, ν_i = 795.9i cm^{-1}), which is much lower than the direct ring-opening reaction in Scheme 3 above (**TS 2–3**, $\Delta\Delta G^{\neq 298}$ = 41.9 kcal mol^{-1}). This implies that it is much easier for **1** to cleave the C2–C3 bond than it is for **2**. We suggest that the large difference in barrier heights is due to the difference of electronic structure between **1** and **2**. The frontier orbitals of **1** and **2** were studied (Supporting Information, S5). The LUMO orbitals are similar in **1** and **2**, but the HOMO orbitals differ a lot. The HOMO orbital in **2** locates on the carboxyl group, so the C2–C3 bond is relatively stable. In **1**, however, the HOMO has a large C2–C3 antibonding component, which explains the fact that the ring cleavage of **1** has much lower barrier than **2**.

Unlike **2**, the removal of the hydroxyl proton essentially makes the pyridine ring atoms and the carboxyl group atoms in **1** lie in the same plane, except for the sp^3-hybridised carbon C2. Our geometry optimisation shows that this chiral carbon C2 is above the ring plane (Figure 5a). When using IRC calculations to trace the product from **TS 1–6a**, we obtain the local minimum **6a′**. This local minimum can easily reach the global minimum **6a** through the C6–N1 single-bond rotation (Supporting Information, S4). The rotation barrier is only 0.2 kcal mol^{-1}, and the free energy difference between **6a′** and **6a** is −3.9 kcal mol^{-1}. In **6a′**, the C2-N1-C6-C5 dihedral angle is −63.1°, whereas in **6a**, all the atoms are in the same plane (C2-N1-C6-C5 dihedral angle −179.9°) to form a large delocalised system, which enhances the stability of **6a** over **6a′**.

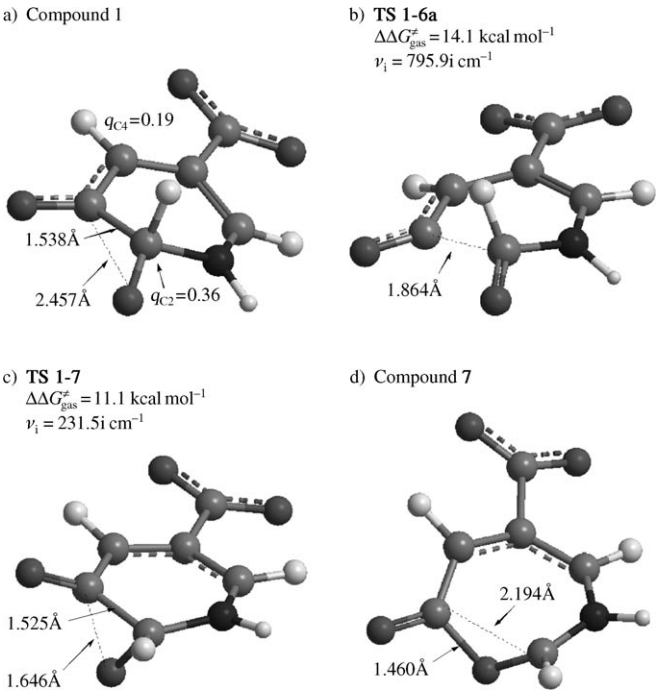

Figure 5. Optimised geometries of important intermediate and transition states in vacuo: a) compound **1**; b) **TS 1–6a**; c) **TS 1–7**; d) compound **7**.

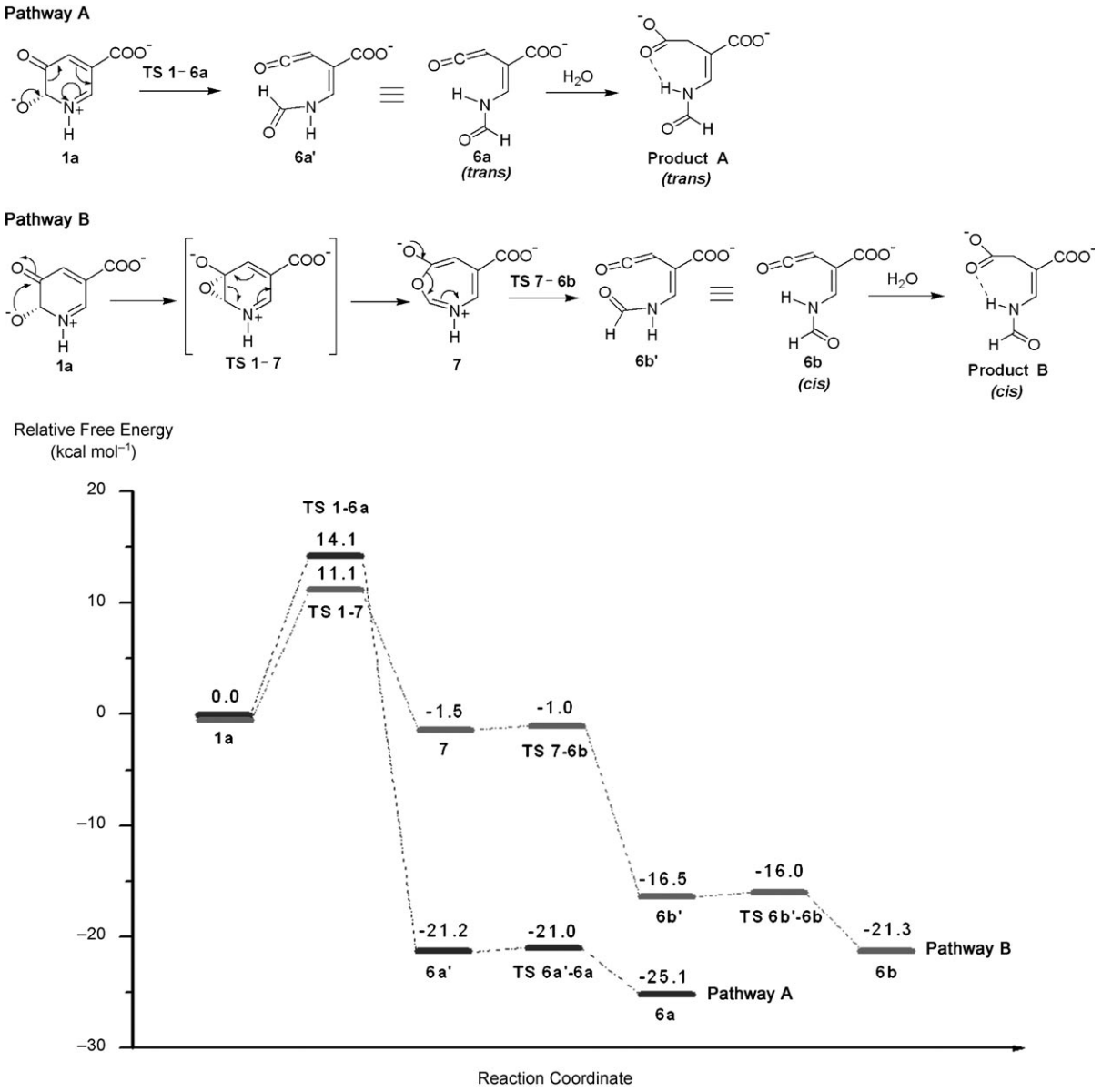

Scheme 4. Current ring-opening pathways. In pathway A, the C2–C3 bond in **1a** cleaves directly to give the ketene intermediate **6a** ($\Delta\Delta G^{\neq 298} = 14.1$ kcal mol^{-1}), which will further be hydrated to form product **A**. In pathway B, **1a** forms intermediate **7** via an epoxy transition state **TS1–7** ($\Delta\Delta G^{\neq 298} = 11.1$ kcal mol^{-1}). With the cleavage of the weak C3–O bond in **7**, **6b** is obtained, which upon hydrolysis gives product **B**.

In pathway B, compound **1** first forms an epoxy transition state (**TS1–7**, $\nu_i = 231.5$i cm^{-1}) to give **7** (Figure 5c–d). The energy barrier is 11.1 kcal mol^{-1}, which is slightly lower than that of pathway A. With the weak C3–O bond broken (**TS7–6b**, $\Delta\Delta G^{\neq 298} = 0.5$ kcal mol^{-1}, $\nu_i = 345.0$i cm^{-1}) we obtain the local minimum **6b′** because the epoxy transition state constrains the direction of the carbonyl C=O bond of the amide pointing towards the ketene group (Figure 5c). The 3 kcal mol^{-1} lower barrier of pathway B implies that it is kinetically favoured compared with pathway A.

We found that in epoxy transition states **TS1–7**, the C2–C3 bond length is shorter than in **1** (1.525 versus 1.538 Å), because during the C3–O bond formation, C2 is pulled back to the pyridine plane (in **1** it is above the plane). Through the rotation of the O=C2–H plane in **1**, the hydrogen on C2 moves to a *cis* position of the hydrogen on N1 (IRC calculation, see Supporting Information S6). This *cis* configuration is maintained in pathway B. The geometry of **TS7–6b** (not shown) is almost the same as **7**, only except for an increase in the C3–O distance (1.460→1.671 Å). In **6b′**, the C2-N1-C6-C5 dihedral angle is 64.7°, which is similar to **6a′** but in opposite direction. The conversion of **6b′** to **6b** is similar to that in pathway A ($\Delta\Delta G^{\neq 298} = 0.5$ kcal mol^{-1}, $\Delta\Delta G^{298}_{\mathbf{6b'-6b}} = -4.9$ kcal mol^{-1}).

C2–N1 bond rotation: It should be noted that in the direct ring-opening process (**TS1–6a**) the two hydrogen atoms on N1 and C2 are in *trans* positions, whereas through the epoxy

transition state (**TS1–7**) the two hydrogen atoms are in *cis* positions (Figure 5b,c). Hence these two pathways reach different configurations of ketene intermediates **6a** and **6b**.

Compounds **6a** and **6b** are stoichiometrically identical, and react with water to give the same carboxylic acid product. However, they give two different configurations of the product (**A** and **B**) that are observable by ^{1}H NMR spectroscopy because the C2−N1 bond rotation in the product is slower than the ^{1}H NMR time scale and the chemical shifts of the hydrogen atoms in **A** and **B** are different.[20] To distinguish between **6a** and **6b**, we introduce the *cis*/*trans* notion, which describes isomers of alkenes; **6a** is labelled *trans* and **6b** is labelled *cis*. The atoms in the amide (OC2-NH-C6) are all in the same plane, again similar to alkenes (Scheme 5).

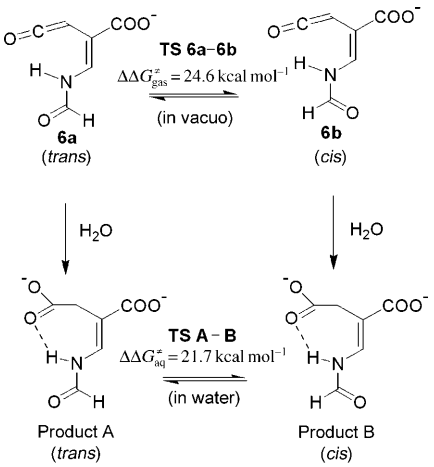

Scheme 5. Product rotations.

The lone pair on N1 is conjugated with the C5=C6 bond, the C2=O bond and also the carboxyl group to form a large delocalised system (O=C2−N1−C6=C5−COO$^-$) in **6a** and **6b**, which restricts the C2−N1 bond rotation. Our calculation shows that the rotation barrier is more than 20 kcal mol^{-1} in vacuo (**6a**→**6b** $\Delta\Delta G^{\neq 298} = 24.6$ kcal mol^{-1}, and **6b**→**6a** $\Delta\Delta G^{\neq 298} = 20.8$ kcal mol^{-1}), implying a slow process. In **TS6a–6b**, the N1 atom adopts an sp^3 configuration rather than the sp^2 configurations in **6a** and **6b**. The O-C2-N1-C6 dihedral angle is −61.9°, and there is little overlap between the π orbital in the aldehyde and the π orbitals in the rest of molecule (Supporting information, S7).

When **6a** and **6b** are released into water, products **A** and **B** are obtained. We found that the hydrogen attached to nitrogen and the newly formed carboxyl interact by a hydrogen bond giving a seven-membered ring, with an O···H distance of 1.85 Å in both **A** and **B** (Supporting Information, S8). As in **6a** and **6b**, the large delocalised system (O=C2−N1−C6=C5−COO$^-$) is present also in **A** and **B**.

Our calculation shows that **A** is 0.6 kcal mol^{-1} higher than **B** in energy, whereas in vacuo **6a** is 3.8 kcal mol^{-1} lower than **6b** in energy. This implies that the environment can affect the preference of different configurations. In Chaiyen's study,[20] the *cis* product **B** is reported to be the major one in D_2O, and the ratio of **B** to **A** is roughly 3:1, which is explained by the current calculations. By using Boltzmann statistics ($e^{-\Delta E/kT}$), an energy difference of 0.6 kcal mol^{-1} corresponds to a 2.8:1 ratio between products **B** and **A** at T= 298 K.

The C2−N1 bond rotation is as slow as that in the ketene intermediates (**A**→**B** $\Delta\Delta G^{\neq 298}_{aq} = 21.7$ kcal mol^{-1}, and **B**→**A** $\Delta\Delta G^{\neq 298}_{aq} = 21.2$ kcal mol^{-1}). In **TS A–B**, the intramolecular hydrogen bond length is shortened (1.859→1.786 Å). The O-C2-N1-C6 dihedral angle is −111.2°, implying poor conjugation between the aldehyde and the C6=C5 double bond.

Alternative ring opening: Besides the two pathways mentioned above, we found that after hydroxylation, the C2−N1 bond in compound **1** can also cleave to give imine product **8** [Eq. (6)].

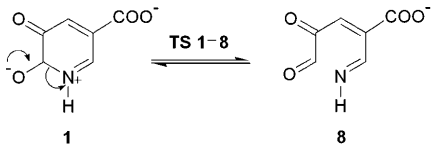

(6)

This conversion is almost barrierless ($\Delta\Delta G^{\neq 298}$ = 0.5 kcal mol^{-1}). However, because the energy difference between **1** and **8** is only 6.9 kcal mol^{-1}, compound **8** can also convert back to **1** ($\Delta\Delta G^{\neq 298} = 7.4$ kcal mol^{-1}). We thus propose that in the enzyme this is a reversible reaction because the energies of the ketene intermediates are much lower than **8** (the energy difference between **8** and **6a** is 18.2 kcal mol^{-1}, and the energy difference between **8** and **6b** is 14.4 kcal mol^{-1}). It should be noted that in principle **8** can also react with water to give α-hydroxyl amine or rearrangement products. Because no such products have been detected, we suggest that water addition probably does not occur in the active site, which is consistent with Scheme 2.

By analysing the reactions of **1** in the presence of FlHOH to mimic the processes in the enzyme active site, we found that FlHOH can stabilise **1**. The barrier heights for conversions of **1** to **6a**, **7** and **8** are increased (Table 1). The structures of the reactant and TS complexes reveal that the most probable reason is the strong hydrogen bond (O···H distance 1.464 Å) formed in complex **III** (Figure 2c). In the transition states of the different pathways, this hydrogen bond is much weaker (Supporting Information, S9). Therefore, the hydrogen-bonding interaction is important for maintaining **1**, and

Table 1. Comparison of the energy barriers for the ring-opening step in the presence of FlHOH.

Conversion	Without FlHOH $\Delta\Delta G^{\neq 298}$ [kcal mol^{-1}]	With FlHOH $\Delta\Delta G^{\neq 298}$ [kcal mol^{-1}]
1→**6a**	14.1	20.7
1→**7**	11.1	16.0
1→**8**	0.5	7.3

affects the barrier heights for the different ring-opening pathways. In the enzyme, the conversions of **1** to **6a** and **6b** might be assisted by the other residues in the active site (work in progress).

Conclusions

The hydroxylation and ring-opening mechanism of MHPCO is studied by computational quantum chemistry. In the hydroxylation, a hydroxyl group is transferred from the activated flavin (FlHOOH) to the substrate through aromatic electrophilic substitution, which is similar to the other aromatic hydroxylases. A barrier height of 33.8 kcal mol^{-1} [MPWB1K/6-31+G(d,p)] is obtained for this step, which is higher than the 24.9 kcal mol^{-1} [B3LYP/6-31+G(d,p)] reported by Bach et al.[26] in a previous study on the PHBH mechanism. The hydroxyl proton is spontaneously transferred back between the hydroxylated substrate and the remaining FlHO$^-$ moiety. Given the small energy difference, both **1** and **2** [Eq. (4)] can be the product of the hydroxylation step; Our calculations show that complex **III** (FlHOH and **1**) is more stable than **II** (FlHO$^-$ and **2**).

The ring opening occurs inside the enzyme active site rather than in water because in water the rearomatisation is predicted to take place immediately, without any barrier, to give an aromatic product. This has, however, not been detected as the product of MHPCO. The instability of the hydroxylated intermediate of MHPCO is the main reason that the acyclic products are formed.

In the ring-cleavage reaction, compound **1** is more likely to cleave the ring than **2** ($\Delta\Delta G^{\neq 298} < 15$ kcal mol^{-1} for **1** versus $\Delta\Delta G^{\neq 298} > 35$ kcal mol^{-1} for **2**). Two possible ring-opening pathways of **1** are found. In pathway A, the ring opens directly ($\Delta\Delta G^{\neq 298} = 14.1$ kcal mol^{-1}) to give **6a**, the *trans* configuration of the ketene intermediate. In pathway B, the *cis* configuration **6b** is obtained by way of an epoxy transition state ($\Delta\Delta G^{\neq 298} = 11.1$ kcal mol^{-1}). The transformation between **6a** and **6b** is restricted ($\Delta\Delta G^{\neq 298} >$ 20 kcal mol^{-1}) due to the large conjugated fragment (O=C2–N1–C6=C5–COO$^-$). The transformation between hydrated product **A** (*trans*) and **B** (*cis*) is slow ($\Delta\Delta G^{\neq 298}_{aq} >$ 20 kcal mol^{-1}), and can be observed by ^{1}H NMR spectroscopy.[20] Our calculations show that **B** is slightly more stable than **A**, which is in accordance with the fact that **B** is the major product. The barrier heights found are in line with those reported for ketosteroid isomerase ($\approx$10.3 kcal mol^{-1}), implying that the rate-limiting step for the current system is indeed the initial hydroxylation rather than the subsequent ring-opening reaction.[43]

The C2–N1 bond in **1** can also be cleaved to give imine **8** ($\Delta\Delta G^{\neq 298} = 0.5$ kcal mol^{-1}). Because no other products than those originating from **6a** and **6b** were detected, and the energy of the ketene products (**6a** and **6b**) are much lower than **8**, this must be a reversible reaction in the enzyme. We furthermore propose that the subsequent water addition probably does not occur in the active site because the reaction of **8** with water would give other products than those detected. FlHOH can stabilise **1** through hydrogen bonding, and the energy barriers are increased for all ring-opening pathways in the presence of FlHOH. This implies that the hydrogen-bonding interaction is important for the ring-opening process.

Acknowledgements

The Swedish Science Research Council (VR), the Faculty of Science and Engineering at Örebro University, and the National University of Ireland—Galway are gratefully acknowledged for financial support.

[1] V. Joosten, W. J. H. Van Berkel, *Curr. Opin. Chem. Biol.* **2007**, *11*, 195.
[2] F. G. Gelalcha, *Chem. Rev.* **2007**, *107*, 3338.
[3] L. De Colibus, A. Mattevi, *Curr. Opin. Struct. Biol.* **2006**, *16*, 722.
[4] W. J. H. Van Berkel, N. M. Kamerbeekb, M. W. Fraaije, *J. Biotechnol.* **2006**, *124*, 670.
[5] M. J. H. Moonen, M. W. Fraaije, I. M. C. M. Rietjens, C. Laane, W. J. H. Van Berkel, *Adv. Synth. Catal.* **2002**, *344*, 1023.
[6] K. McCulloch, T. Mukherjee, T. Begley, S. Ealick, *Biochemistry* **2009**, *48*, 4139.
[7] H. A. Schreuder, P. A. J. Prick, R. K. Wierenga, G. Vriend, K. S. Wilson, W. G. J. Hol, J. Drenth, *J. Mol. Biol.* **1989**, *208*, 679.
[8] C. Enroth, H. Neujahr, G. Schneider, Y. Lindqvist, *Structure* **1998**, *6*, 605.
[9] N. Treiber, G. E. Schulz, *J. Mol. Biol.* **2008**, *379*, 94.
[10] B. A. Palfey, D. P. Ballou, V. Massey in *Active Oxygen: Reactive Oxygen Species in Biochemistry* (Eds.: J. S. Valentine, J. F. Liebman), Chapman-Hall, Glasgow, **1996**, pp. 37–83.
[11] B. Entsch, W. J. H. Van Berkel, *FASEB J.* **1995**, *9*, 476.
[12] M. Ortiz-Maldonado, D. P. Ballou, V. Massey, *Biochemistry* **1999**, *38*, 8124.
[13] P. Chaiyen, J. Sucharitakul, J. Svasti, B. Entsch, V. Massey, D. P. Ballou, *Biochemistry* **2004**, *43*, 3933.
[14] W. Oonanant, J. Sucharitakul, J. Yuvaniyama, P. Chaiyen, *Acta. Crystallogr. Sect. F* **2005**, *61*, 312.
[15] P. Chaiyen, P. Brissette, D. P. Ballou, V. Massey, *Biochemistry* **1997**, *36*, 2612.
[16] P. Chaiyen, D. P. Ballou, V. Massey, *Proc. Natl. Acad. Sci. USA* **1997**, *94*, 7233.
[17] G. M. Kishore, E. E. Snell, *J. Biol. Chem.* **1981**, *256*, 4228.
[18] G. M. Kishore, E. E. Snell, *J. Biol. Chem.* **1981**, *256*, 4234.
[19] P. Chaiyen, P. Brissette, D. P. Ballou, V. Massey, *Biochemistry* **1997**, *36*, 8060.
[20] P. Chaiyen, P. Brissette, D. P. Ballou, V. Massey, *Biochemistry* **1997**, *36*, 13856.
[21] L. G. Sparrow, P. P. K. Ho, T. K. Sundaram, D. Zach, E. J. Nyns, E. E. Snell, *J. Biol. Chem.* **1969**, *244*, 2590.
[22] E. J. Nyns, D. Zach, E. E. Snell, *J. Biol. Chem.* **1969**, *244*, 2601.
[23] R. W. Burg, V. W. Rodwell, E. E. Snell, *J. Biol. Chem.* **1960**, *235*, 1164.
[24] M. J. K. Nelson, E. E. Snell, *J. Biol. Chem.* **1986**, *261*, 15115.
[25] J. Sucharitakul, M. Prongjit, D. Haltrich, P. Chaiyen, *Biochemistry* **2008**, *47*, 8485.
[26] R. D. Bach, O. Dmitrenko, *J. Am. Chem. Soc.* **2004**, *126*, 127.
[27] R. D. Bach, O. Dmitrenko, *J. Phys. Chem. B* **2003**, *107*, 12851.
[28] C. Canepa, R. D. Bach, O. Dmitrenko, *J. Org. Chem.* **2002**, *67*, 8653.
[29] R. D. Bach, M. D. Su, *J. Am. Chem. Soc.* **1994**, *116*, 5392.
[30] L. Ridder, A. J. Mulholland, J. Vervoort, I. M. C. M. Rietjens, *J. Am. Chem. Soc.* **1998**, *120*, 7641.
[31] L. Ridder, A. J. Mulholland, I. M. C. M. Rietjens, J. Vervoort, *J. Am. Chem. Soc.* **2000**, *122*, 8728.

[32] L. Ridder, J. N. Harvey, I. M. C. M. Rietjens, J. Vervoort, A. J. Mulholland, *J. Phys. Chem. B* **2003**, *107*, 2118–2126.
[33] H. M. Senn, S. Thiel, W. Thiel, *J. Chem. Theory Comput.* **2005**, *1*, 494.
[34] Y. Zhao, D. G. Truhlar, *J. Phys. Chem. A* **2004**, *108*, 6908.
[35] A. D. Becke, *Phys. Rev. A* **1988**, *38*, 3098.
[36] A. D. Becke, *J. Chem. Phys.* **1993**, *98*, 5648.
[37] C. Lee, W. Yang, R. G. Parr, *Phys. Rev. B* **1988**, *37*, 785.
[38] B. Mennucci, J. Tomasi, *J. Chem. Phys.* **1997**, *106*, 5151.
[39] J. Tomasi, B. Mennucci, E. Cances, *J. Mol. Struct.* **1999**, *474–515*, 211.
[40] Gaussian 03, Revision B.01, M. J. Frisch, G. W. Trucks, H. B. Schlegel, G. E. Scuseria, M. A. Robb, J. R. Cheeseman, J. A. Montgomery, Jr., K. N. Kudin, J. C. Burant, J. M. Millam, S. S. Iyengar, J. Tomasi, V. Barone, B. Mennucci, M. Cossi, G. Scalmani, N. Rega, G. A. Petersson, H. Nakatsuji, M. Hada, M. Ehara, K. Toyota, R. Fukuda, J. Hasegawa, M. Ishida, T. Nakajima, Y. Honda, O. Kitao, H. Nakai, M. Klene, X. Li, J. E. Knox, H. P. Hratchian, J. B. Cross, C. Adamo, J. Jaramillo, R. Gomperts, R. E. Stratmann, O. Yazyev, A. J. Austin, R. Cammi, C. Pomelli, J. W. Ochterski, P. Y. Ayala, K. Morokuma, G. A. Voth, P. Salvador, J. J. Dannenberg, G. Zakrzewski, S. Dapprich, A. D. Daniels, M. C. Strain, O. Farkas, D. K. Malick, A. D. Rabuck, K. Raghavachari, J. B. Foresman, J. V. Ortiz, Q. Cui, A. G. Baboul, S. Clifford, J. Cioslowski, B. B. Stefanov, G. Liu, A. Liashenko, P. Piskorz, I. Komaromi, R. L. Martin, D. J. Fox, T. Keith, MvA. Al-Laham, C. Peng, Y. A. Nanayakkara, M. Challacombe, P. M. W. Gill, B. Johnson, W. Chen, M. Wong, W. C. Gonzalez, J. A. Pople, Gaussian Inc.: Pittsburgh, PA, **2003**.
[41] B. Entsch, B. A. Palfey, D. P. Ballou, V. Massey, *J. Biol. Chem.* **1991**, *266*, 17341.
[42] The charges on the carbon atoms are Mulliken atomic charges with hydrogen atoms summed into the heavy atoms.
[43] D. C. Hawkinson, T. C. M. Eames, R. M. Pollack, *Biochemistry* **1991**, *30*, 10849.

Received: August 13, 2009
Published online: January 11, 2010

